

See discussions, stats, and author profiles for this publication at: <https://www.researchgate.net/publication/230765070>

Hydrogenation of Ferrimagnetic Graphene on Co Surface: Significant Enhancement of Spin Moment by C-H Functionality

ARTICLE in JOURNAL OF PHYSICAL CHEMISTRY LETTERS · AUGUST 2012

Impact Factor: 7.46 · DOI: 10.1021/jz3010283

CITATIONS

4

READS

106

4 AUTHORS:



Indu Kaul

Indian Institute of Science Education and Re...

4 PUBLICATIONS 27 CITATIONS

[SEE PROFILE](#)



Niharika Joshi

Indian Institute of Science Education and Re...

4 PUBLICATIONS 21 CITATIONS

[SEE PROFILE](#)



Nirmalya Ballav

Indian Institute of Science Education and Re...

85 PUBLICATIONS 1,529 CITATIONS

[SEE PROFILE](#)



Prasenjit Ghosh

Indian Institute of Science Education and Re...

25 PUBLICATIONS 210 CITATIONS

[SEE PROFILE](#)

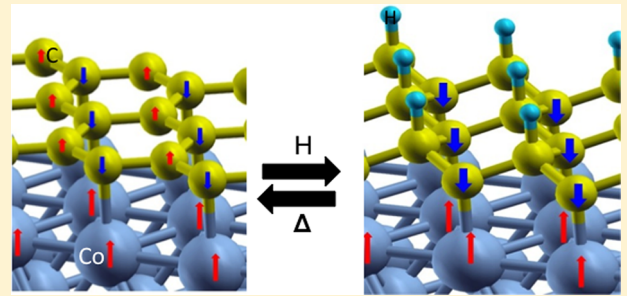
Hydrogenation of Ferrimagnetic Graphene on a Co Surface: Significant Enhancement of Spin Moments by C–H Functionality

Indu Kaul,[†] Niharika Joshi,[‡] Nirmalya Ballav,[†] and Prasenjit Ghosh*,^{†,‡}

[†]Department of Chemistry and [‡]Department of Physics, Indian Institute of Science Education and Research, Pune-411021, India

ABSTRACT: Using ab initio density functional theory, we present a novel way of simultaneously enhancing the induced magnetic moment and opening up the band gap of a graphene sheet supported on ferromagnetic transition metal surface. Specifically, we have demonstrated that by simply hydrogenating graphene supported on ferromagnetic Co surface at saturation coverage, (i) there is a six-fold increase in the magnitude of the induced magnetic moment compared with the pristine graphene on the Co surface and (ii) for both the spin-up and the spin-down channels there is a band gap opening at the K-point of the Brillouin zone.

SECTION: Surfaces, Interfaces, Porous Materials, and Catalysis



Magnetism in materials has usually been associated with systems containing unpaired localized d or f electrons. Over the past decade there has been a lot of debate regarding magnetism in carbon (C)-based materials where there are s and p electrons.^{1,2} Recently, magnetism has been found in different C-based materials. For example, Ohldag et al.³ have shown that proton-irradiated graphite is magnetic, where the cause for the magnetism has been attributed to the presence of defects due to irradiation.⁴ In lower dimension systems, for example, zigzag-edged graphene nanoflakes have also been predicted to be magnetic.⁵

In addition to the intriguing fact that magnetism is observed (or predicted) in different forms of graphene, its unique electronic structure gives rise to exceptional transport and spin-filtering properties, making it a promising candidate for applications in graphene based electronic devices.⁶ However, graphene is a semimetal with the conduction and valence band forming the Dirac cone at the K-point of the Brillouin zone (BZ). To use graphene as a material for semiconductor spintronics, it is desirable not only to make graphene magnetic but also to open up the band gap. It has been recently shown that covalent functionalization of graphene⁷ or noncovalent stacking with aromatic molecules through π – π interactions can be used to open the band gap.^{8,9} Moreover, for any device application of graphene, making contacts with metals is necessary. In particular, growth of graphene on Ni(111) and Co(0001) surfaces is particularly interesting because of the almost perfect lattice matching between the substrate (Ni or Co surfaces) and the graphene sheet. The lattice matching enables growth of stable epitaxial overlayers without the formation of complex superstructures, which are the results of large lattice mismatch. Recent studies of the electronic and magnetic properties of graphene supported on Ni(111) surface by Weser et al.¹⁰ have shown that there is a weak induced magnetic moment ($0.01 \mu_B$) in the graphene sheet. To use the induced

magnetic properties of graphene for device applications, it is desirable to increase the magnitude of the induced magnetic moment. On intercalating a Fe monolayer in between Ni(111) surface and graphene, one can slightly increase the induced magnetic moments. Whereas the magnetic moments of the two inequivalent C atoms in the absence of Fe are 0.031 and $-0.019 \mu_B$, upon intercalating Fe, the magnetic moments increase to -0.050 and $0.039 \mu_B$.¹¹

Although there have been many studies (both experimental and theoretical) on Ni(111)/graphene interfaces, graphene on Co(0001) is almost unexplored.¹² Compared with Ni (bulk magnetic moment of $0.62 \mu_B$ per Ni atom), the magnetic moment of Co atoms (bulk magnetic moment of $1.69 \mu_B$ per Co atom) is much higher. Therefore one might expect that the magnitude of the induced magnetic moments on graphene supported on Co(0001) might be much higher than those on Ni(111) surface. In this letter, using ab-initio-based density functional theory (DFT), we report our detailed investigations of the electronic and magnetic properties of graphene supported on Co(0001) surface. We also propose an effective way (through chemical functionalization) to (i) significantly enhance the induced magnetic moment in the graphene sheet supported on Co(0001) surface and (ii) open up of the band gap at the K-point of the BZ, which is experimentally achievable.

The calculations are performed using Quantum Espresso software,¹³ which is an implementation of DFT with a plane-wave basis set. Electron–ion interactions are described using ultrasoft pseudo potentials.¹⁴ We have used a kinetic energy cut off of 30 and 300 Ry for wave functions and charge density,

Received: July 24, 2012

Accepted: August 29, 2012

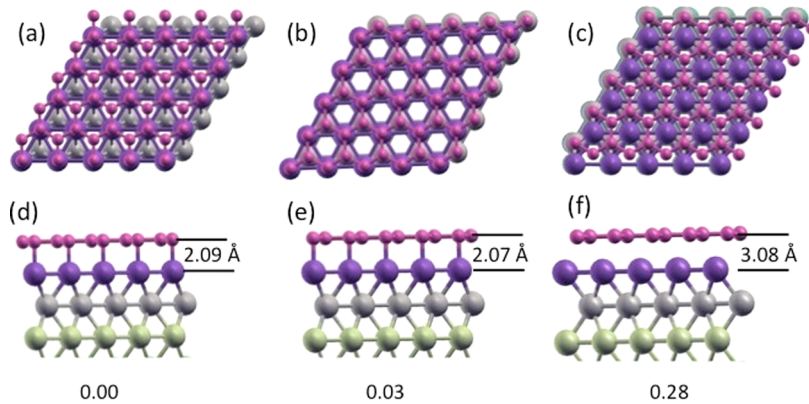


Figure 1. Top and side view of graphene on Co(0001) in *top-fcc* (a,d), *top-hcp* (b,e), and *fcc-hcp* (c,f) configurations. The numbers given below each configuration show the energy difference between the different configurations, with the *top-fcc* configuration being lowest in energy and indicated by 0.00. All energies are in electronvolts.

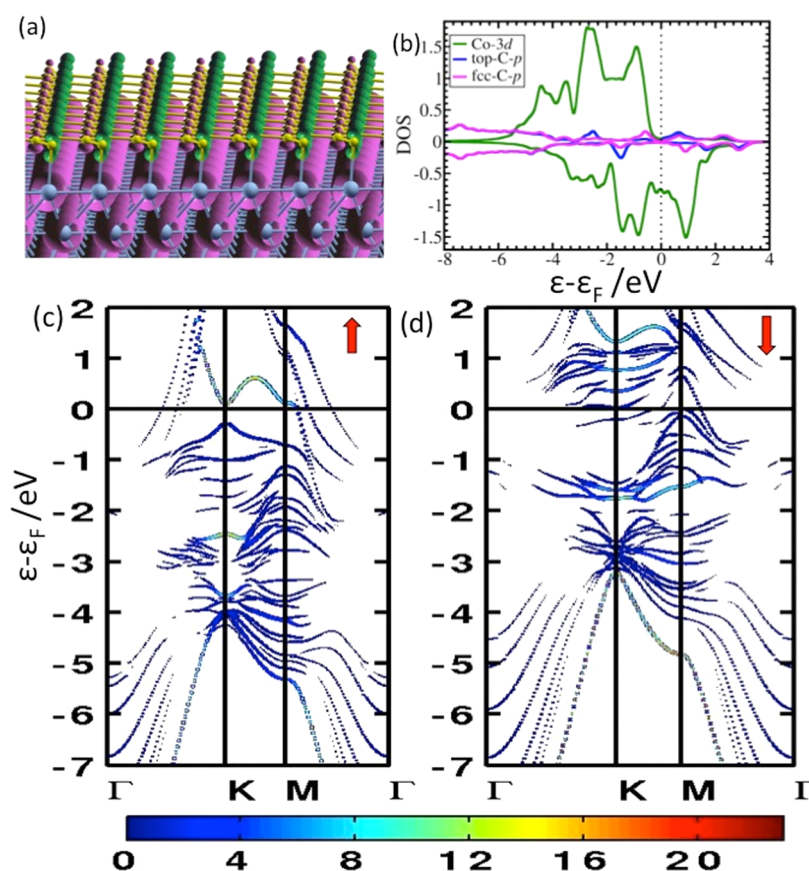


Figure 2. Magnetization density isosurfaces (a) and the projected density of states plot (b) of the *top-fcc* configuration of graphene on Co(0001) surface. Magenta (green) isosurfaces denote spin-up (down) magnetization density. (c,d) Contour plots of the contribution of the top and fcc C-p_z orbitals to the total density of states for spin-up and spin-down, respectively, along the high-symmetry directions of the BZ.

respectively. The electron–electron exchange and correlation are described using Perdew, Burke, and Ernzerhof parametrization-based generalized gradient approximation (GGA-PBE).¹⁵ BZ integrations have been done with a (34 × 34 × 1) Monkhorst-Pack *k*-point mesh.¹⁶ To speed up the convergence, we have used Marzari–Vanderbilt smearing¹⁷ with a smearing width of 0.01 Ry. For bulk Co, we obtain a lattice parameter of 2.50 Å, a c/a ratio of 1.55, and a magnetic moment of 1.69 μ_B per Co atom, which are in good agreement with the previous reports.^{18,19} The lattice parameter of graphene (2.46 Å)

obtained from our calculations is also in excellent agreement with previous calculations and experimental measurements.²⁰

The Co(0001) surface is modeled with an asymmetric slab consisting of seven layers of Co, where the bottom three layers are kept fixed at the bulk interplanar separation and the remaining four layers are relaxed. The fixed bottom layer is passivated with Cu atoms to quench the *spurious magnetization*. To avoid the interaction between the periodic images, a vacuum of ~10 Å is used. In practice, when graphene is grown on a substrate, the graphene sheet is strained by the substrate potential. The amount of strain depends on the degree of lattice

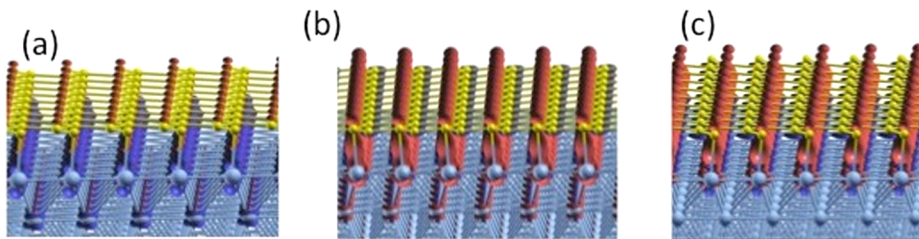


Figure 3. Isosurfaces corresponding to spin resolved ((a) for spin-up and (b) for spin-down) and total (c) charge transfer between graphene and Co(0001) for an isovalue of 0.03 electrons/ \AA^3 . The charge transfer is given by $\rho^\sigma(r) = \rho^\sigma(r)_{\text{Co+Graphene}} - \rho^\sigma(r)_{\text{Co}} - \rho^\sigma(r)_{\text{Graphene}}$, where σ denotes spin-up or spin-down and $\rho(r)$ denotes the charge density at r . Red (green) isosurfaces denote charge accumulation (depletion).

mismatch. In the case of Co(0001) surface, there is an almost perfect lattice matching with graphene. Hence the graphene sheet is expected to grow pseudomorphically on the Co substrate. Therefore, to study the interactions of graphene sheet with the Co substrate, both the graphene and Co substrate are kept at the Co(0001) lattice parameter of 2.50 \AA . Dispersion interactions play an important role in graphene–transition metal interfaces, which is not taken into account by conventional PBE exchange correlation functional. Therefore, we have included an empirical vdW (van der Waals) correction to account for the dispersive interactions.^{21,22} However, we note that this is an empirical correction to the total energy and it does not affect the magnetic couplings of the system.

We considered three possible configurations, namely, *top-fcc*, *top-hcp*, and *hcp-fcc*. In *top-fcc* (Figure 1a,d), one of the C atoms is directly above the Co atom of the topmost layer and the second C atom is at the void fcc site. For the *top-hcp* configuration (Figure 1b,e), one of the C atoms is situated above the Co atoms of the first layer (top site), whereas the other is on the top of the Co atom in the second layer (hcp site). In *hcp-fcc* (Figure 1c,f), the two C atoms are placed on hcp and fcc sites, respectively. Our calculations show that graphene shows the strongest binding with the Co substrate in the *top-fcc* configuration, the binding energy of the graphene sheet being -0.22 eV/C atom. A comparison of the binding energy without including van der Waals interaction shows that the contribution of van der Waals interaction to the binding energy is -0.2 eV/C atom, suggesting that the binding of the graphene sheet with Co is predominantly due to van der Waals interaction. The Co–C distance is 2.1 \AA , and we do not observe any buckling of the graphene sheet. Our results are in excellent agreement with previous reported results.^{23,24} However, the energy difference between the *top-fcc* and *top-hcp* configurations is quite small. Therefore, it is not possible to say conclusively whether graphene would be in the *top-fcc* or the *top-hcp* configuration. We note that the STM measurements of graphene on Co(0001) by Eom et al. also could not conclusively show whether graphene would prefer to be on the *top-fcc* or the *top-hcp* configuration. Further experiments and calculations that can capture the effects of the local coordination (for e.g. C-1s core level X-ray absorption spectra) are needed to decide conclusively which of the two configurations is preferred or whether both of them coexist. Because from our calculations the *top-fcc* configuration is lowest in energy, we have used this configuration for the hydrogenation study.²⁵

Figure 2a shows the calculated magnetization density plot for the *top-fcc* configuration. We find that there is an induced magnetic moment in the graphene sheet. The top-C atoms have a magnetic moment of $-0.083 \mu_B$ and are aligned

antiparallel to those on the Co atoms. The C atoms on the fcc sites have a magnetic moment of $0.059 \mu_B$ and are aligned parallel to the Co atoms. Hence graphene turns ferrimagnetic with an average magnetic moment of $-0.024 \mu_B$. The magnetic moment of Co top layer is quenched from $1.78 \mu_B$ per surface Co atom for the clean surface to $1.54 \mu_B$.

To understand the origin of the induced magnetic moment, we calculated the projected density of states (PDOS) and the k -point resolved PDOS (KPDOS). The contour plots of the KPDOS along the high-symmetry directions of the BZ give the contribution from each atom to the band structure. The PDOS (Figure 2b) shows strong hybridization of the C-2p states of graphene and Co-3d states that lead to splitting of spin-up and spin-down states of the C atoms. This is also evident from the KPDOS for the spin-up and spin-down channels, as shown in Figure 2c,d, respectively. Because of the interaction between the substrate and the graphene states, the Dirac cone at the K-point of the BZ (which is a characteristic feature of the electronic structure of graphene) is destroyed, resulting in a slight opening of the band gap at the K-point (0.38 eV for spin-up and 0.24 eV for spin-down). For the spin-up channel, at the K-point of the BZ, the states at 0.10 eV and -2.45 eV (Figure 2c) results from the interaction of top-C- p_z states with the Co- d_z^2 states. Because the fcc-C atom occupies the hollow site formed by the three surface Co atoms, the p_z states of the fcc-C interact more strongly with the Co d_{zx} , d_{zy} , $d_{x^2-y^2}$, and d_{xy} states. These interactions give rise to new states at -0.27 (primarily from interaction primarily with the Co d_{zx} , d_{zy} states), -1.0 , -1.40 , and -1.72 eV (these states are due to interactions primarily with the Co $d_{x^2-y^2}$ and d_{xy} states), as shown in Figure 2c. Similar features are also observed for the spin-down channel, as shown in Figure 2d. However, in this case, the states are moved much higher in energy.

This hybridization results in charge transfer between the Co atoms and the graphene sheet. Figure 3 shows spin-resolved charge-transfer isosurfaces for graphene–Co(0001) interface. For the clean Co surface, the 3d spin-up (spin-down) states are completely (partially) filled. Therefore, when graphene interacts with Co, there is a transfer of spin-up electrons from the Co d states to the p states of the fcc-C atoms. There is also slight accumulation of spin-up charge in between the top-C atoms of graphene and the surface Co atoms (Figure 3a). For the spin-down electrons, there is both donation and back-donation of electrons between the graphene sheet and the Co substrate (Figure 3b). The net effect of this spin-resolved charge redistribution (Figure 3c) is that the majority of the electrons accumulated on the fcc-C (top-C) atoms are predominantly spin-up (down), resulting in the net magnetic moment on the fcc-C (top-C) atom to be aligned parallel (antiparallel) to those on the Co atoms. Moreover, Figure 3c

also shows that the fcc-C atoms are electron-deficient sites, whereas the top-C atoms are electron-rich sites.

Upon hydrogenating the graphene supported on the Co surface with 0.5 ML of hydrogen (where 1 ML means one H atom per graphene C atom), H can bind either on the top or on the fcc-C atoms. We find that H prefers to bind to the fcc-C atom with a binding energy²⁶ of -2.04 eV/H atom. This is 0.1 eV stronger than the binding of the H atom to the top-C atoms. H forms strong covalent bonds with the fcc-C atoms, which, as mentioned in the previous paragraph, are the electron-deficient sites and therefore the more preferred site. To estimate the stability of the semihydrogenated graphene sheet, we have calculated its binding energy with and without van der Waals interaction. The binding energies are about -1.80 and $-1.16 \text{ eV}/(1 \times 1)$ unit cell, respectively, and thus for semi-hydrogenated graphene, van der Waals interaction is not as dominant as for the pristine graphene. The contribution of van der Waals interaction to the binding energy is $-0.64 \text{ eV}/(1 \times 1)$ unit cell. To accommodate the H atoms, the graphene lattice tends to undergo an expansion,²⁷ which, in the present case, it is unable to do because it is constrained by the substrate potential. As a result, hydrogenation results in strong buckling of the graphene sheet. The fcc-C atoms move away from the substrate, whereas the top-C atoms move toward the surface. The C–C interplanar separation is 0.44 Å, and the C–H bond distance is 1.13 Å.

The magnetization density and the PDOS of the graphene sheet on Co(0001) after hydrogenation are shown in Figure 4a,b, respectively. Hydrogenation of the graphene sheet results in the following two effects. First, the H-atom forms strong σ

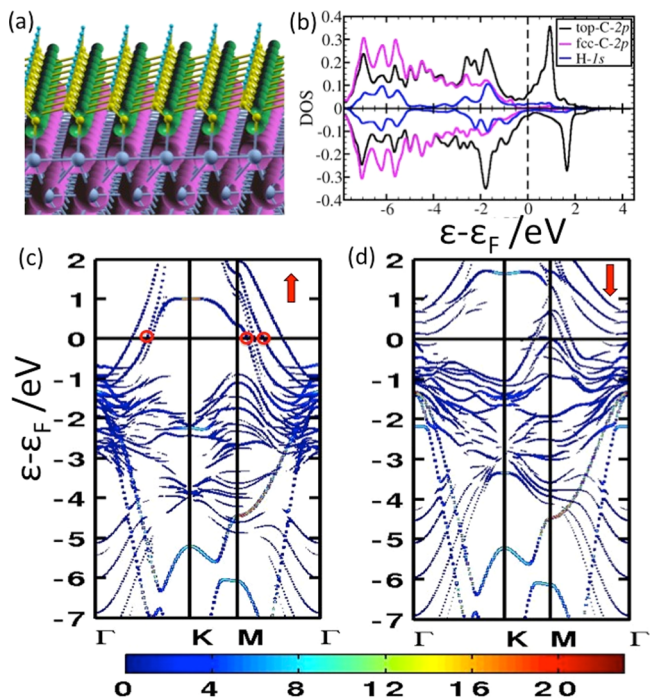


Figure 4. Magnetization density isosurfaces (a) and the projected density of states plot (b) of hydrogenated graphene on Co(0001) surface. Magenta (green) isosurfaces denote spin-up (down) magnetization density. (c,d) Contour plots of the contribution of the top and fcc C-p_z orbitals to the total density of states for spin-up and spin-down, respectively, along the high-symmetry directions of the BZ. The red circles in panel c denote the states that have a p character.

bonds with the fcc-C atoms of graphene, resulting in significant quenching of the magnetic moment of the fcc-C atom (from $0.059 \mu_B$ to $0.01 \mu_B$). We also observe slight magnetic moment on the H atom ($0.02 \mu_B$). Second, because of the formation of the σ -bonds between the fcc-C atoms and H, the π electron cloud on the top-C atom is further localized. This results in increase in the magnetic moment on the top-C atom from $-0.083 \mu_B$ to $-0.15 \mu_B$. However, unlike graphene (free-standing semi hydrogenated graphene), the electrons in the unhydrogenated top-C atoms of the graphene sheet supported on Co(0001) surface are not completely localized due to the interaction with the Co substrate. This results in smaller magnitude of the magnetic moment compared with free-standing graphene. Like the supported graphene sheet, the hydrogenated graphene sheet becomes ferrimagnetic, but now with an average magnetic moment of $-0.14 \mu_B$, aligned antiparallelly with respect to Co. Thus chemical modification of the graphene sheet through hydrogenation results in a six-fold increase in magnetic moment of the graphene sheet. Note that for graphene and hydrogenated graphene supported on fcc-Co(111) surface we have found similar results.

Figure 4c,d shows the KPDOS of the hydrogenated graphene along the high-symmetry directions of the BZ. In addition to the increase in the magnitude of the magnetic moment, hydrogenation of the supported graphene sheet results in further opening up of the band gap at the K-point of the BZ. For the spin-up states, the band gap at the K-point is $\sim 3.19 \text{ eV}$, whereas for the spin-down states it is $\sim 2.64 \text{ eV}$. Moreover, unlike free-standing graphene, the electronic states for both the spin-up and spin-down electrons cross the Fermi energy at other points of the BZ. This is due to the strong sp-d hybridization. We analyzed the wave functions corresponding to these states. Whereas for the spin-up channel there are three states (marked by red circles in Figure 4c), which has significant p character coming from the C atoms of graphene, for the spin-down channels, all states crossing the Fermi energy have a predominantly Co-d character. Therefore, when using this interface in a device, whereas the spin-up channel of the supported hydrogenated graphene sheet will be conducting, the spin-down channel may be insulating. This might enable more efficient spin filtering when these interfaces will be used in spintronic devices.

As for the experimental feasibility, single-layer graphene can be easily prepared on a metallic thin film Co substrate,²⁸ and subsequent basal-plane hydrogenation (at saturated coverage) can be performed either by low-pressure dc plasma discharge of a hydrogen–argon mixture²⁹ or by a commercially available Omicron EFM H source.²⁸ Considering the reactivity of active hydrogen atoms (radicals), one would expect equal probability of the covalent attachment to both the top and the fcc C atoms as far as the kinetic factor dominates. However, hydrogenation predominantly on the fcc-C atoms, which is thermodynamically favorable as suggested by our calculations, can be achieved by controlling reaction parameters like temperature, partial pressure (hydrogen dosage), and time. Furthermore, dehydrogenation could be achieved upon simple annealing of the sample at 450°C in an inert atmosphere.²⁹ Thereby, our presented approach of tuning the interfacial magnetochemical effect in ferrimagnetic graphene is apparently reversible. We also note that the induced magnetic moment in graphene on ferromagnetic Ni surface, even though very small (on the order of 0.05 to $0.1 \mu_B$), was successfully estimated by employing X-ray magnetic circular dichroism (XMCD) spectroscopy^{10,11} and

spin-resolved photoemission spectroscopy (PES).³⁰ Here the proposed six-fold enhancement in the magnetic moment in graphene on ferromagnetic Co surface by hydrogenation is also anticipated to be measured by similar surface-sensitive spectroscopic techniques (XMCD or PES).

In conclusion, we have studied in detail the electronic and magnetic properties of graphene supported on Co(0001) surface. Our calculations show that there is an induced magnetic moment in the graphene sheet whose origin we attribute to the different charge transfer of the spin-up and the spin-down electrons. The graphene sheet becomes ferrimagnetic with an average magnetic moment of $-0.024 \mu_B$, aligned antiparallel with respect to that of the Co substrate. Upon hydrogenating the graphene sheet at saturation coverage, there is a six-fold increase in the average magnetic moment of the graphene sheet. Considering the feasibility, we hope our results will motivate experimental studies on the proposed system.

AUTHOR INFORMATION

Corresponding Author

*E-mail: pghosh@iiserpune.ac.in, prasenjit.jnc@gmail.com.

Notes

The authors declare no competing financial interest.

ACKNOWLEDGMENTS

We would like to thank IISER Pune and Centre for Development of Advanced Computing, Pune, India for providing the HPC facility to do the calculations. I.K. and N.J. have equal contributions in this work.

REFERENCES

- (1) Fan, X. F.; Liu, L.; Wu, R. Q.; Peng, G. W.; Fan, H. M.; Feng, Y. P.; Kuo, J.-L.; Shen, Z. X. The Role of sp-Hybridized Atoms in Carbon Ferromagnetism: A Spin-Polarized Density Functional Theory Calculation. *J. Phys.: Condens. Matter* **2010**, *22*, 046001–1–7.
- (2) Yazyev, O. V. Emergence of Magnetism in Graphene Materials and Nanostructures. *Rep. Prog. Phys.* **2010**, *73*, 056501–1–16.
- (3) Ohldag, H.; Tyliszczak, T.; Hohne, R.; Spemann, D.; Esquinazi, P.; Ungureanu, M.; Butz, T. π -Electron Ferromagnetism in Metal-Free Carbon Probed by Soft X-Ray Dichroism. *Phys. Rev. Lett.* **2007**, *98*, 187204–1–4.
- (4) Duplock, E. J.; Scheffler, M.; Lindan, P. J. D. Hallmark of Perfect Graphene. *Phys. Rev. Lett.* **2004**, *92*, 225502–1–4.
- (5) Wang, B.; Bocquet, M. L.; Marchini, S.; Guenther, S.; Wintterlin, J. Chemical Origin of A Graphene Moiré Overlayer on Ru(0001). *Phys. Chem. Chem. Phys.* **2008**, *10*, 3530–3534.
- (6) Karpan, V. M.; Giovannetti, G.; Khomyakov, P. A.; Talanana, M.; Starikov, A. A.; Zwierzyczyk, M.; van den Brink, J.; Brocks, G.; Kelly, P. J. Graphite and Graphene as Perfect Spin Filters. *Phys. Rev. Lett.* **2007**, *99*, 176602–1–4.
- (7) Englert, J. M.; Dotzer, C.; Yang, G.; Schmid, M.; Papp, C.; Gottfried, J. M.; Steinrück, H. P.; Specker, E.; Hauke, F.; Hirsch, A. Covalent Bulk Functionalization of Graphene. *Nat. Chem.* **2011**, *3*, 279–286.
- (8) Kozlov, S. M.; Viñes, F.; Görling, A. Bandgap Engineering of Graphene by Physisorbed Adsorbates. *Adv. Mater.* **2011**, *23*, 2638–2643.
- (9) Zhang, Z.; Huang, H.; Yang, X.; Zang, L. Tailoring Electronic Properties of Graphene by π – π Stacking with Aromatic Molecules. *J. Phys. Chem. Lett.* **2011**, *2*, 2897–2905.
- (10) Weser, M.; Rehder, Y.; Horn, K.; Sicot, M.; Fonin, M.; Preobrajenski, A. B.; Voloshina, E. N.; Goering, E.; Dedkov, Y. S. Induced Magnetism of Carbon Atoms at the Graphene/Ni(111) Interface. *Appl. Phys. Lett.* **2010**, *96*, 012504–1–3.
- (11) Weser, M.; Voloshina, E. N.; Horn, K.; Dedkov, Y. S. Electronic Structure and Magnetic Properties of the Graphene/Fe/Ni(111) Intercalation-Like System. *Phys. Chem. Chem. Phys.* **2011**, *13*, 7534–7539.
- (12) Eom, D.; Prezzi, D.; Taeg Rim, K.; Zhou, H.; Lefenfeld, M.; Xiao, S.; Nuckolls, C.; Hybertsen, M. S.; Heinz, T. F.; Flynn, G. W. Structure and Electronic Properties of Graphene Nanoislands on Co(0001). *Nano Lett.* **2009**, *9*, 2844–2848.
- (13) Giannozzi, P.; Baroni, S.; Bonini, N.; Calandra, M.; Car, R.; Cavazzoni, C.; Ceresoli, D.; Chiarotti, G. L.; Cococcioni, M.; Dabo, I.; et al. Quantum Espresso: A Modular and Open-Source Software Project for Quantum Simulations of Materials. *J. Phys.: Condens. Matter* **2009**, *21*, 395502–1–19.
- (14) Vanderbilt, D. Soft Self-Consistent Pseudopotentials in a Generalized Eigenvalue Formalism. *Phys. Rev. B* **1990**, *41*, 7892–7895.
- (15) Perdew, J. P.; Burke, K.; Ernzerhof, M. Generalized Gradient Approximation Made Simple. *Phys. Rev. Lett.* **1996**, *77*, 3865–3868.
- (16) Monkhorst, H. J.; Pack, J. D. Special Points for Brillouin-Zone Integrations. *Phys. Rev. B* **1976**, *13*, 5188–5192.
- (17) Marzari, N.; Vanderbilt, D.; DeVita, A.; Payne, M. C. Thermal Contraction and Disordering of the Al(110) Surface. *Phys. Rev. Lett.* **1999**, *82*, 3296–3299.
- (18) Wyckoff, R. W. G. *The Structure of Crystals*, 2nd ed.; American Chemical Society Monograph Series; The Chemical Catalog: New-York, 1931; p 1.
- (19) Iota, V.; Klepeis, J. P.; Yoo, C.; Lang, J.; Haskel, D.; Srajer, G. Electronic Structure and Magnetism in Compressed 3d Transition Metals. *Appl. Phys. Lett.* **2007**, *90*, 042505–1–3.
- (20) Moodera, J. S.; Kinder, L. R.; Wong, T. M. Large Magnetoresistance at Room Temperature in Ferromagnetic Thin Film Tunnel Junctions. *Phys. Rev. Lett.* **1995**, *74*, 3273–3276.
- (21) Grimme, S. Semiempirical GGA-Type Density Functional Constructed with a Long-Range Dispersion Correction. *J. Comput. Chem.* **2006**, *27*, 1787–1799.
- (22) Barone, V.; Casarin, M.; Forrer, D.; Pavone, M.; Sambi, M.; Vittadini, A. Role and Effective Treatment of Dispersive Forces in Materials: Polyethylene and Graphite Crystals as Test Cases. *J. Comput. Chem.* **2009**, *30*, 934–939.
- (23) Swart, J. C. W.; van Steen, E.; Ciobă, I. M.; van Santen, R. A. Interaction of Graphene with fcc-Co(111). *Phys. Chem. Chem. Phys.* **2009**, *11*, 803–807.
- (24) Mohn, P. *Magnetism in the Solid State*; Springer-Verlag: Berlin, 2003; p 134.
- (25) We note that the differences in energies between the top-fcc and top-hcp configurations are within the error bar of the calculations. Hence we cannot conclusively say which one of them is the preferred configuration. For the hydrogenation studies, we have done calculations for both the above-mentioned configurations. For both of the systems we obtained similar results. Because the top-fcc configuration is lowest in energy, in the rest of the letter, we have presented the results on the hydrogenation performed with the top-fcc configuration.
- (26) The binding energy has been considered with respect to the energy of the H atom in the gas phase because in experiments atomic H is supplied to the graphene sheet.
- (27) Zhou, J.; Wang, Q.; Sun, Q.; Chen, X. S.; Kawazoe, Y.; Jena, P. Ferromagnetism in Semihydrogenated Graphene Sheet. *Nano Lett.* **2009**, *9*, 3867–3870.
- (28) Ng, M. L.; Balog, R.; Hornekær, L.; Preobrajenski, A. B.; Vinogradov, N. A.; Mårtensson, N.; Schulte, K. Controlling Hydrogenation of Graphene on Transition Metals. *J. Phys. Chem. C* **2010**, *114*, 18559–18565.
- (29) Elias, D. C.; Nair, R. R.; Mohiuddin, T. M. G.; Morozov, S. V.; Blake, P.; Halsall, M. P.; Ferrari, A. C.; Boukhvalov, D. W.; Katsnelson, M. I.; Geim, A. K.; et al. Control of Graphene's Properties by Reversible Hydrogenation: Evidence for Graphane. *Science* **2009**, *323*, 610–613.

- (30) Dedkov, Y. S.; Fonin, M. Electronic and Magnetic Properties of the Graphene-Ferromagnet Interface. *New J. Phys.* **2010**, *12*, 125004–1–22.